



Impacts of temperature and soil characteristics on methane production and oxidation in Arctic polygonal tundra

Jianqiu Zheng¹, Taniya RoyChowdhury^{1,2}, Ziming Yang^{3,4}, Baohua Gu³, Stan D. Wullschleger^{3,5}, David E. Graham^{1,5}

5 ¹ Biosciences Division, Oak Ridge National Laboratory, Oak Ridge, Tennessee, 37831, USA

² Now at Department of Environmental Science & Technology, University of Maryland, College Park, Maryland, 20742, USA

³ Environmental Sciences Division, Oak Ridge National Laboratory, Oak Ridge, Tennessee, 37831, USA

⁴ Now at Department of Chemistry, Oakland University, Rochester, Michigan, 48309, USA

10 ⁵ Climate Change Science Institute, Oak Ridge National Laboratory, Oak Ridge, Tennessee, 37831, USA

Correspondence to: David E. Graham (grahamde@ornl.gov)

This manuscript has been authored by UT-Battelle, LLC under Contract No. DE-AC05-00OR22725 with the U.S.
15 Department of Energy. The United States Government retains and the publisher, by accepting the article for publication, acknowledges that the United States Government retains a non-exclusive, paid-up, irrevocable, world-wide license to publish or reproduce the published form of this manuscript, or allow others to do so, for United States Government purposes. The Department of Energy will provide public access to these results of federally sponsored research in accordance with the DOE Public Access Plan (<http://energy.gov/downloads/doe-public-access-plan>).

20

Abstract

Methane (CH₄) oxidation mitigates CH₄ emission from soils. However, it is still highly uncertain whether soils in high-latitude ecosystems will function as a net source or sink for this important greenhouse gas. We investigated CH₄ production and oxidation potential in permafrost-affected soils from degraded ice-wedge polygons with carbon-rich soils at the Barrow
25 Environmental Observatory, Utqiagvik (Barrow) Alaska, USA. Frozen soil cores from flat and high-centered polygons were sectioned into active layers, transition zones, and permafrost, and incubated at -2, +4 and +8°C to determine potential CH₄ production and oxidation rates. Organic acids produced by fermentation fueled methanogenesis and competing iron reduction processes responsible for most anaerobic respiration. Significant CH₄ oxidation was observed from the suboxic transition zone and permafrost of flat-centered polygon soil, which also exhibited higher CH₄ production rates during the
30 incubations. Although CH₄ production showed higher temperature sensitivity than CH₄ oxidation, potential rates of CH₄ oxidation exceeded methanogenesis rates at each temperature. Assuming no diffusion limitation, our results suggest that CH₄



oxidation could offset CH₄ production and limit surface CH₄ emissions, in response to elevated temperature, and thus should be considered in model predictions of net CH₄ fluxes in Arctic polygonal tundra.

1 Introduction

5 Arctic ecosystems store vast amounts of organic carbon in active layer soils and permafrost (Hugelius et al., 2014; Shiklomanov et al., 2010). Warmer air temperatures are increasing soil temperatures, annual thaw depths, and length of the thaw season, exposing more of this carbon to microbial degradation and mineralization (Shiklomanov et al., 2010; Schuur et al., 2015; Schuur et al., 2013). The potential carbon loss due to these direct effects is estimated to be 92±17 Pg carbon over the coming century (Schuur et al., 2015). In addition, thawing of ground ice and ice-wedge degradation cause ground
10 subsidence and significant changes in soil water saturation (Liljedahl et al., 2016), which could alter the future fluxes of carbon dioxide (CO₂) and methane (CH₄) to the atmosphere (Schädel et al., 2016). Understanding the factors that control these fluxes is key to predicting the greenhouse gas feedback on a future warming climate.

Arctic tundra acts as a large net source of CH₄, with a current estimation of the source strength ranging widely from 8 to 29
15 Tg C yr⁻¹ (McGuire et al., 2012). The large uncertainty associated with this estimation is due to the spatial and temporal complexity of the Arctic ecosystem. The unique polygonal ground in Arctic coastal plain tundra creates natural gradients in hydrology, snow pack depth and density, and soil organic carbon storage that control CH₄ fluxes (Liljedahl et al., 2016; Lara et al., 2015). Thermal contraction processes create cracks in the tundra soil, which can fill with water that freezes to produce massive ground ice (French, 2007). This ice forms wedges that create the borders of three dominant polygon types, defined
20 by their surface relief and subsurface hydrology: low-centered polygons (LCPs), flat-centered polygons (FCPs), and high-centered polygons (HCPs) (MacKay, 2000). Poorly drained LCPs are characterized by wet centers bordered by raised, relatively dry rims and wet troughs. FCPs lack the rims of LCPs and are drier (Wainwright et al., 2015). When ice wedges erode and water drains from the polygons, troughs subside and rims disappear to form drier HCPs. Methane emissions from wet and inundated LCP sites were about one order of magnitude higher than emissions from drier FCP and HCP sites
25 (Vaughn et al., 2016; Sachs et al., 2010). Although a number of factors, including vegetation height and plant composition (von Fischer et al., 2010), soil inundation (Sturtevant et al., 2012), thaw depth (Sturtevant and Oechel, 2013; Grant et al., 2017), and season (Chang et al., 2014) were suggested as explanatory factors for CH₄ flux variations, the huge differences in CH₄ flux between polygon types could not be fully explained by variations in moisture or temperature (Sachs et al., 2010; Vaughn et al., 2016). High concentrations of dissolved CH₄ in the deeper active layer, contrasted with low surface emissions
30 from FCPs and HCPs, suggest the importance of methane oxidation in these landscape features might be underestimated (Vaughn et al., 2016).



Soil CH₄ fluxes result from the net effect of microbial CH₄ production and oxidation, coupled with transport processes. Soils at the Barrow Environmental Observatory in Utqiagvik (Barrow), Alaska experience a wide range of arctic temperatures, from -20 to +4°C (Shiklomanov et al., 2010). Soil respiration and methanogenesis continue at low temperatures close to 0 °C, even after the soil surface freezes trapping gas under ice. Therefore, substantial annual CH₄ and CO₂ emissions from the Alaskan Arctic occur during the spring thaw (Commane et al., 2017; Raz-Yaseef et al., 2017; Zona et al., 2016). However, it is unclear how rapid temperature change in Arctic soils affects the opposing processes of CH₄ production and oxidation due to their nonlinear response to temperature fluctuations (Treat et al., 2015).

Methane oxidation mitigates terrestrial CH₄ emission. Up to 90% of CH₄ produced in the soil is consumed in the upper dry layers of soil by aerobic CH₄-oxidizing bacteria (methanotrophs) before reaching the atmosphere (Le Mer and Roger, 2001). High-affinity methanotrophs oxidize substantial amounts of atmospheric methane in high Arctic mineral soils (Lau et al., 2015). Methane oxidation rates are usually greatest in oxic, surficial soils, and methane oxidation is known to occur under oxygen-limiting conditions as well (Roslev and King, 1996). In the classical model of CH₄ oxidation profiles, there is usually a vertical gradient of decreasing O₂ concentration in the top cm of the soil column that is inversely correlated with an increasing gradient of CH₄ through the suboxic/anoxic active layer. The relative abundance of methanotrophs generally correlates with CH₄ oxidation activity at the soil surface, and methanogens are relatively abundant in the deeper layer where oxygen is limiting (Lee et al., 2015). Methane oxidation potential in peat bogs is highest immediately above the water table, while most CH₄ is produced below the water table (Whalen and Reeburgh, 2000). In contrast, methanogenic and methanotrophic communities can overlap in the rhizosphere (Liebner et al., 2012; Knoblauch et al., 2015), where roots or *Sphagnum* create an oxic/anoxic interface providing a substantial amount of oxygen for methanotrophs (Laanbroek, 2010; Parmentier et al., 2011) and organic substrates for methanogenesis. The rates of CH₄ oxidation are mainly governed by the abundance and composition of methanotrophic microbial communities and environmental factors including CH₄ and O₂ availability, soil air-filled porosity and soil-water content (Preuss et al., 2013). Previous studies of boreal lakes and wetlands showed that CH₄ production is more sensitive to temperature fluctuations than CH₄ oxidation, as CH₄ oxidation rates respond more rapidly to CH₄ availability than temperature increase (Liikanen et al., 2002; Segers, 1998). However, most temperature sensitivity measurements for CH₄ processes have been performed at mesophilic temperatures that are higher than typical Arctic soil temperatures.

Various studies have identified correlated factors affecting CH₄ and CO₂ production in permafrost ecosystems upon thawing, but the oxidation of CH₄ is not considered in most incubation studies (Treat et al., 2015). The coupled response of methanogenesis and CH₄ oxidation to increased temperature is poorly understood. Similarly, the role of fermenters that produce organic acid substrates for competing processes of methanogenesis and iron reduction is not well characterized. To improve estimates of CH₄ production from soils across the permafrost zone, additional research on rates of CH₄ oxidation is needed to scale up results from laboratory studies and to better constrain CH₄ budgets from permafrost region. In this study,



we use the natural geomorphic gradient of FCP and HCP soils to explore the soil organic carbon decomposition pathways and specifically test the following hypotheses based on temperate ecosystem CH₄ dynamics to explain CH₄ production in organic Arctic soils.

- 5 (1) CH₄ production is localized in the oxygen-depleted subsurface while CH₄ oxidation occurs in the surface layers of oxic soil.
- (2) CH₄ production is more sensitive to temperature increase than CH₄ oxidation and will likely exceed CH₄ oxidation in wet areas in response to warming.

2 Materials and Methods

10 2.1 Site description and soil sampling

The study site is located at the Barrow Environmental Observatory (BEO), Utqiagvik (Barrow), Alaska as part of the Intensive Study Site areas B (High-Centered Polygon, HCP) and C (Flat-Centered Polygon, FCP) of the Next Generation Ecosystem Experiments (NGEE) in the Arctic project. The centers of HCPs in area B were covered by lichens, moss and dry tundra graminoids, while centers of FCPs in area C hosted wet tundra graminoids, mosses and bare ground (Langford et al.,
15 2016). Intact frozen soil cores from the centers of a water-saturated FCP (N 71° 16.791', W 156° 35.990') and a well-drained HCP (N 71° 16.757', W 156° 36.288') were collected with a modified SIPRE auger containing a sterilized liner, driven by a hydraulic drill during a field campaign in April 2012 (Herndon et al., 2015a; Herndon et al., 2015b; Roy Chowdhury et al., 2015). All samples were kept frozen during core retrieval, storage and shipment to Oak Ridge National Laboratory (ORNL, Oak Ridge, TN). The frozen cores were stored at -20 °C until processing. The thaw depth measured in September 2012 in the
20 HCP center was 40 cm, and thaw depths in the FCP varied from 41-47 cm.

The frozen soil cores were inspected and processed inside an anaerobic chamber (Coy Laboratories, MI. H₂ ≤ 2% and O₂ < 1 ppm). The soil core collected from the FCP center showed evidence of discontinuous organic matter depositions below the active layer mineral horizon and above the permafrost. This transition zone from 40-50 cm between active layer and
25 permafrost was attributed to episodic thawing and cryoturbation (Schoor et al., 2008; Bockheim, 2007). No equivalent transition zone was identified in the HCP core. Both cores were sectioned into layers of 10-cm increments, and each section was inspected for evidences of roots, undecomposed organic matter, and soil Munsell color recorded to qualitatively infer redoximorphic features. Gravimetric water content, pH in a potassium chloride slurry (pH_{KCl}), Fe(II) concentration, total carbon and nitrogen were measured in each section as described previously (Roy Chowdhury et al., 2015), and pore water
30 gas concentrations were measured using the method described in Sect. 2.2.



Based on similarities in the above mentioned geochemical properties, several soil sections were combined to represent the active layer, transition zone and upper permafrost. The top 10 cm of the cores contained substantial ice or plant material; these sections were not used for soil incubation studies. The next two sections (comprising 10-30 cm depth) were combined to represent the active layer, for both FCP and HCP cores. The FCP section from 40-50 cm depth provided transition zone samples. Finally, sections from 50-70 cm depth were combined to represent permafrost layer soils for both cores. Soils from each layer were homogenized inside the anaerobic chamber using sterile tools and equipment. The homogenized soil from each layer was sub-sampled for microcosm incubation studies described below.

2.2 Soil pore water gas measurements

Dissolved gas (CO_2 and CH_4) concentrations in soil pore water were determined at each 10-cm depth-interval from the FCP and HCP cores. A 1:1 (w:v) soil slurry was prepared by mixing 10 g wet soil in 10 mL de-ionized and de-gassed water under anoxic conditions inside an anaerobic chamber. The samples were then placed in 15 mL crimp-sealed serum vials (Wheaton, NJ). Vials were inverted and shaken at 4 °C for 12 h to allow for exchange between the dissolved and soil gas phases. Then, ~5 mL of the aqueous phase was exchanged with Ar (99.9 % purity) using a Gastight syringe (Hamilton, NV), and samples were manually shaken vigorously for 5 min to allow for equilibration between the aqueous and gas phase. Subsequently, a 500- μL headspace sample was drawn and immediately analyzed with an SRI 8610C gas chromatograph using the method previously described (Roy Chowdhury et al., 2015). The detection limit for CH_4 was 1 ppm_v. Concentrations of CH_4 and CO_2 were corrected for dissolved gases based upon temperature and pH-dependent Henry's Law constants (Sander, 2015).

2.3 Soil microcosm setup, methane oxidation potential assay and soil chemical analyses

2.3.1 Temperature sensitivity of CO_2 and CH_4 production from unamended microcosms

To investigate the temperature response of CH_4 production and overall organic carbon mineralization rates (measured as CO_2 production), homogenized soils described in section 2.1 from the FCP or HCP active layer, transition zone (only in FCP), and permafrost were used in incubations (Table S1). Replicate (n=9) microcosms of each homogenized soil layer were constructed in sterile 70 mL serum bottles sealed with blue butyl stoppers and aluminum crimps. Soils from FCP and HCP core layers were incubated under anoxic or oxic conditions, determined by the concentrations of reduced Fe(II) measured in each layer (Howeler and Bouldin, 1971). Microcosms from active layers of both FCP and HCP cores were prepared in oxic conditions with ambient laboratory air. Microcosms from the transition zone and permafrost of FCP and the permafrost layer of HCP were set up inside the anaerobic chamber. Microcosms were flushed with N_2 three times after sealing to remove residual H_2 and O_2 from the headspace. All microcosms contained ~10 g wet soil, and they were incubated at -2, +4 or +8 °C for approximately 90 days. It is important to note that at -2 °C soil water remained unfrozen in these samples due to freezing point depression (Romanovsky and Osterkamp, 2000).



2.3.2 Methane oxidation potential assay

Soil samples were incubated in oxic conditions supplemented with ample CH₄ substrate to measure CH₄ oxidation potential (Roy Chowdhury et al., 2014). After 0, 10 or 20 days of microcosm incubation described in section 2.3.1, three replicates corresponding to each layer and temperature were opened to set up CH₄ methane oxidation assays and further analyses.

- 5 Replicate (n=9) samples (about 2 g) from each time point were slurried in a 1:1 (w:v) ratio with autoclaved de-ionized water in 26 mL serum bottles under oxic conditions. A 1% CH₄ headspace was introduced into each crimp-sealed bottle by replacing 0.23 mL headspace with 99.99% CH₄. Samples were incubated at the same incubation temperature as the microcosms from which they were harvested. To eliminate gas-liquid phase transfer limitation, samples from FCP were shaken and incubated at 4 °C, and samples from HCP were shaken and incubated at 8 °C. Headspace CO₂ and CH₄
- 10 concentrations in soil incubations and methane oxidation assays were measured at 2 to 15 days' time intervals using gas chromatography as described in section 2.2.

2.3.3 Extractable ion analysis

Aliquots of soil samples from microcosms opened after 10, 20 and 90 days of incubation were extracted with either 10 mM NH₄HCO₃ (pH ~ 7.3) or 0.1 M KCl (pH~ 5.0) solution for determining soil organic acids and extractable Fe(II), respectively. Briefly, NH₄HCO₃ extractions (12 h) were centrifuged for 15 min at 6500 g, and the supernatants were further filtered through 0.2 µm membrane filters before analysis. Filtered sample were analyzed for low-molecular-weight organic acids using a Dionex ICS-5000⁺ system (Thermo Fisher Scientific, MA) equipped with an IonPac AS11-HC column with a KOH mobile phase. Fe(II) concentrations from filtered KCl extract samples were diluted and quantified using the HACH Ferrous method 8146 (1,10-phenanthroline). Absorbance was measured at 510 nm using a DU 800 spectrophotometer (Beckman Coulter, CA). Soil pH was determined using the slurry method by mixing a 1:5, w:v ratio of soil to 1M KCl.

2.4 Rate estimation, temperature sensitivity and statistical analyses

Concentrations of CH₄ and CO₂ accumulated over time in soil microcosms were fitted with hyperbolic, sigmoidal, or linear functions (Roy Chowdhury et al., 2015). Rates of CO₂ production were calculated using derivatives of the best curve-fitting equations with parameters listed in Table S1. To estimate temperature sensitivity, gas production rates at -2, +4, and +8 °C were fit to the exponential Arrhenius equation, and a quotient of rates (Q₁₀) is calculated as described previously (Roy Chowdhury et al., 2015). Methane oxidation rates were calculated from the loss of headspace CH₄, which were best fitted with simple linear regression. All rate calculations are reported on per gram soil dry mass basis.

- 30 Changes of soil physicochemical properties were evaluated with one-way ANOVA, Tukey's Honest Significant Difference (HSD) test. The effect of soil layers (active, transition zone and permafrost) and incubation temperature (-2, 4 and 8 °C) were



examined with Tukey's HSD test. All curve fittings and statistical analyses are performed with R 3.4.0 (The R Foundation for Statistical Computing) and validated with Prism (GraphPad Software, ver. 7.0a).

2.5 Calculation of net CH₄ emission

Representation of CH₄ oxidation is based on Michaelis-Menten kinetics with a linear dependence on the biomass of methanotrophs in Eq. (1) (Xu et al., 2015), while the CH₄ production rate is calculated from measurements directly using Eq. (2).

$$R_{oxi} = B_{methanotrophs} \cdot V_{max,oxi} \left[\frac{C_{CH_4}}{C_{CH_4} + K_{m,CH_4}} \right] \left[\frac{C_{O_2}}{C_{O_2} + K_{m,O_2}} \right] \quad (1)$$

$$R_{pro} = B_{methanogens} \cdot V_{measure,pro} \quad (2)$$

where $B_{methanotrophs}$ and $B_{methanogens}$ represent the estimated biomass of methanotrophs and methanogens respectively. K_{m,CH_4} and K_{m,O_2} are the half saturation coefficients (mM) with respect to CH₄ and O₂ concentrations, respectively. Values of K_{m,CH_4} and K_{m,O_2} are 0.005 and 0.02, with ranges of 0.0005-0.05, 0.002-0.2, respectively (Riley et al., 2011). The maximum CH₄ oxidation rate $V_{max,oxi}$ and CH₄ production rate $V_{measure,pro}$ were obtained from the incubations. By assuming $R_{oxi} = R_{pro}$, the ratio of $B_{methanogens}$ to $B_{methanotrophs}$ can be calculated at different temperatures. Initial CH₄ and O₂ concentrations were calculated from soil porewater dissolved gas measurement and soil air-filled porosity estimations.

3 Results

3.1 Soil attributes and pore water characteristics

Soil cores from FCP and HCP center positions showed distinct vertical profiles of soil moisture expressed as gravimetric water content (g g⁻¹ dry soil). The soil core from FCP was characterized by a wet surface within the top 10 cm below ground, a much drier intermediate layer between 10 to 40 cm, and a bottom layer below 40 cm with significantly higher water content (Fig. 1). A similar water distribution has been recorded by continuous field measurements of volumetric water content at the nearby NGEE_BRW_C soil pit monitoring site (<http://permafrostwatch.org>). Soil moisture from the HCP core gradually increased from the top to the bottom (Fig. 1), consistent with field measurements of the water level in nearby HCPs (Liljedahl et al., 2016). Fe(II) concentration showed a strong positive correlation with gravimetric water content in both FCP and HCP cores ($R^2=0.81$, and $R^2=0.91$, respectively). The soil pH in FCP increased steadily with soil depth ($R^2=0.95$), with an average of 4.7. In the soil core of HCP, soil pH varied by 1.5 pH unit, with an average of 5.4. Overall, soil moisture, Fe(II) concentration and pH increased with depth in the centers of both polygon types.



Dissolved CO₂ in soil pore water showed a similar general trend in both FCP and HCP cores. The concentration of dissolved CO₂ was between 0.2 to 0.6 μmol g⁻¹ dry soil in the first 40 cm and 0.9 to 1.6 μmol g⁻¹ dry soil below 50 cm. The highest dissolved CH₄ concentration was found between 40 to 50 cm in soil pore water of FCP, approximately 4 times the CH₄ concentration measured from the top 10 cm (Fig. 1). Significant CH₄ accumulation in soil pore water was found below 50 cm of the HCP core, while no dissolved CH₄ was detected above 50 cm. The active layers of FCP and HCP cores were both oxidic, with low Fe(II) concentrations and minimal dissolved CH₄ in soil pore water, while deeper layers were more reduced and suboxic with significantly higher Fe(II) concentrations and dissolved CH₄ (Fig. S1).

The total carbon content of the FCP permafrost (31%) was nearly 66% greater than the active layer content and five-fold more than the transition zone (Table S1). The total carbon content of active and permafrost layers of HCP were 21% and 17%, respectively, and substantially lower than that of the FCP permafrost. Inorganic carbon quantified as CO₂ released upon acid treatment was less than 0.001% for all layers of the FCP and HCP cores.

3.2 CH₄ production and oxidation rates

3.2.1 CH₄ production

Thawed FCP and HCP soil samples were incubated in microcosms at fixed temperatures to assess methanogenesis rates. To emulate the natural redox gradient, FCP and HCP active layer samples were incubated in oxidic conditions, while transition zone and permafrost samples were incubated in anoxic conditions, as described in Sect. 2.3.1. CH₄ production was only observed in microcosms from the transition zone and permafrost of FCP, which were incubated under anoxic conditions. CH₄ production was detected within 5 days after the anoxic incubations were set up (Fig. 2). Cumulative CH₄ concentrations at all temperatures were best fitted with a linear model (Table S2). Samples from the transition zone yielded about 10 times more CH₄ than permafrost layer samples.

CH₄ concentrations measured from both HCP layers, and the active layer of FCP were all below the detection limit of 1 ppm_v (Fig. S2). Methanogenesis was unlikely to occur in the active layers from FCP and HCP as these microcosms were incubated under oxidic conditions, and our calculation suggested that O₂ was not completely consumed after 90 days incubation (data not shown).

3.2.2 Methane oxidation potential

Potential rates of aerobic CH₄ oxidation were measured as described in Sect. 2.3.2 using freshly thawed soils (0 day and 5 days) and soils that had been previously incubated (10 days and 20 days pre-incubation) in the microcosms described in Sect.



2.3.1. Potential CH₄ oxidation rates in HCP soils were 80-90% lower than rates from the equivalent FCP soil layers (Fig. 3). CH₄ oxidation potentials from transition zone and permafrost soils were more than twofold higher than the active layer in freshly thawed FCP samples (Fig. 3a). Similar to FCP soils, freshly thawed HCP permafrost showed slightly higher CH₄ oxidation potentials than active layer soil (Fig. 3c).

5

Pre-incubated soils from FCP microcosms showed similar CH₄ oxidation potentials to newly thawed soils at +8 °C (Fig. 3). However, the potential increased significantly in transition zone samples incubated at -2 °C ($p=0.01$), perhaps due to methanotroph biomass increasing in response to methanogenesis during the 20 day pre-incubation. HCP permafrost layer samples obtained after 10 days of anoxic incubation also show higher CH₄ oxidation potentials ($p<0.05$, Fig. 3c, 3d).

10

3.3 Temperature sensitivity of CH₄ production and oxidation

Potential CH₄ production rates from both transition zone and permafrost of FCP were significantly higher at +8 °C than -2 °C ($p < 0.01$, t-test). Transition zone soil showed a stronger temperature response, with a Q₁₀ value of 4.2 ± 0.9 , compared to 1.7 ± 0.7 for permafrost.

15

The temperature dependency of CH₄ oxidation was consistent among soils layers. CH₄ oxidation potentials significantly increased when the incubation temperature increased from -2 to +8 °C in active layer soil ($p < 0.01$), with a Q₁₀ value of 1.7 ± 0.3 . Potential rates also increased with temperature for the transition zone and permafrost soils despite more variability: Q₁₀ values were 2.0 ± 1.6 and 1.7 ± 0.5 , respectively. HCP samples had relatively low rates of CH₄ oxidation. Significant temperature response was observed in pre-incubated permafrost samples from HCP microcosms ($p=0.01$). This soil sample also demonstrated the greatest temperature sensitivity, with a Q₁₀ value of 6.1 ± 1.7 .

20

3.4 CO₂ production and its temperature sensitivity

Soils in all of the microcosm incubations produced CO₂, by aerobic respiration under oxic conditions or by anaerobic respiration and fermentation under anoxic conditions. CO₂ production started immediately (day 1) in microcosms of FCP samples (Fig. 4). Soils from the active layer were incubated under initial oxic conditions, and these oxic soils produced 10 times more CO₂ after prolonged incubations compared to soils from transition zone and permafrost samples that were incubated under anoxic conditions. CO₂ accumulation was best modelled by a hyperbolic function, except the active layer soil incubated at -2 or +4 °C where the best fit was a linear function (Table S3, Fig. 4). This exception is likely due to continuous aerobic respiration at lower temperatures, indicating that substrate limitation was not reached within 90 days. The transition zone had the slowest CO₂ production rates and least carbon loss via CO₂, in contrast to its relatively high rate of methanogenesis.

30



CO₂ production in microcosms of HCP samples showed a different pattern from FCP samples. For active layer soils, the cumulative CO₂ production from aerobic incubations of HCP soils was an order of magnitude lower than FCP soils, despite similar total C content (Fig. 4). The same difference in cumulative CO₂ production was also observed from permafrost incubated under anoxic conditions. The HCP cumulative CO₂ production profiles were best fitted with a sigmoidal model, compared to the hyperbolic model that best fit FCP data (Table S3). A prolonged delay in CO₂ accumulation was observed in both HCP active and permafrost layer samples. CO₂ production started about 10 days after the microcosm setup in the active layer and reached a maximum rate at 30 days (+4 and +8 °C) or 75 days (-2 °C). The delay was longer in permafrost incubations, with a rapid increase after 40 to 50 days followed by a plateau. Therefore, microorganisms mineralized more carbon from FCP soils than HCP soils, and CO₂ production began sooner in FCP than HCP soil incubations.

Temperature showed significant effects on CO₂ production from the active layer and transition zone of FCP during 90 day incubations ($p < 0.01$ for each layer) (Fig. 4). FCP soils incubated at +8 °C produced substantially more CO₂ than those incubated at lower temperatures. In the permafrost layer of FCP, CO₂ production was significantly higher at +8 °C compared to 2 °C ($p < 0.05$, ANOVA with Tukey's multiple comparisons test). The temperature sensitivity for CO₂ production in FCP soils was highest for oxic active layer FCP samples ($Q_{10} = 5.8 \pm 1.8$) and lower for anoxic transition zone and permafrost samples ($Q_{10} = 0.9 \pm 0.6$ and 2.2 ± 1.0 , respectively estimated for day 1). The Q_{10} values of HCP active and permafrost layers could not be readily estimated from sigmoidal models due to different lag periods, but were empirically estimated at 2.7 ± 0.02 and 2.6 ± 1 , respectively. Therefore, the FCP active layer aerobic mineralization was most sensitive to a temperature rise, while the anaerobic processes in the transition zone and permafrost had a temperature sensitivity typical of many soils (discussed below).

3.5 Organic acids production and iron reduction in FCP soils

Organic acids were produced as intermediate metabolites during microbial degradation of organic matter, and they probably fueled methanogenesis and iron reduction. Specific organic acids were analyzed from soil extracts from FCP transition zone and permafrost (Table 1). The most abundant organic acids included formate, acetate, propionate, butyrate, and oxalate, consistent with previous analyses from LCP soils (Herndon et al., 2015a). Trace amount of lactate, pyruvate, and succinate were detected, with concentrations less than 0.05 μmol g⁻¹ soil. Concentrations of dominant organic acids measured in the permafrost were approximately 10 times higher than those measured in the transition zone. The difference was associated with lower total carbon content (5.8%) in the transition zone than that in the permafrost (30.8%). Significant increases in acetate concentration after the incubation were observed from both transition zone ($p = 0.02$) and permafrost ($p = 0.02$) layers, while formate and propionate decreased by up to 40% in both layers.



Incubation temperature showed a profound impact on the acetate dynamics. In the transition zone, acetate concentration increased by 56%, 142%, and 156% at -2, 4, and 8 °C, respectively after the incubation. Acetate concentrations in permafrost samples increased from high initial values by 17%, 39% and 53%, respectively.

- 5 To compare the changes in organic acids over time, total organic carbon contained in formate, acetate, propionate, butyrate and oxalate products was calculated (T_{OA} , $\mu\text{mol C g}^{-1}$), and the changes during the incubation were plotted for each layer of FCP (Fig. 5). T_{OA} drastically dropped to near zero in the active layer due to the aerobic decomposition. Under anaerobic conditions, T_{OA} generally increased during the incubations, except for permafrost incubated at 4 °C.
- 10 Significant changes in Fe(II) concentrations were observed from anoxic incubations of FCP samples over the incubation period (Fig. 6). In the transition zone, Fe(II) concentrations stayed at initial levels during the first 20 days of anoxic incubation, and then increased significantly from $\sim 50 \mu\text{mol g}^{-1}$ to $\sim 100 \mu\text{mol g}^{-1}$ during the 20 to 90 days incubation period at -2, 4 and 8 °C. In the permafrost, the highest level of iron reduction within the first 20 days was observed in samples incubated at -2 °C. Between 20 and 90 days, the highest iron reduction rates were observed in samples incubated at 8 °C.
- 15 The estimated Q_{10} values were 1.2 and 1.3 for transition zone and permafrost, respectively. If we assume that iron reduction is coupled to acetate oxidation to produce CO_2 , stoichiometric calculations suggest that iron reduction could account for 96% and 70% of CO_2 produced in the transition zone and permafrost at -2 °C. At 8 °C iron reduction could account for 74% and 61% of acetate oxidation in the transition zone and permafrost, respectively.

20 4 Discussion

- The widespread ice-wedge degradation in the Arctic causes morphological succession and hydrological changes in tundra ecosystems (Liljedahl et al., 2016). FCP and HCP features represent successively more degraded polygons. Despite clear geomorphological differences between polygon types that affect drainage, vegetation and snow cover, the FCP and HCP active layers were similar in terms of their gravimetric water contents, pH, SOC, and Fe(II) concentrations. Permafrost from
- 25 both polygons contains more water, dissolved CH_4 and Fe(II) than active layer soils indicating more reducing environments. Concentrations of CH_4 measured in soil pore water from FCP and HCP cores increased with depth. These results are consistent with field measurements of dissolved CH_4 in soil pore water sampled using piezometers during the thaw season (Herndon et al., 2015b). The disconnect between CH_4 trapped in the permafrost layer and trace amounts of dissolved CH_4 in active layer samples suggests CH_4 oxidation in the upper active layer. Therefore, we began this work with the following
 - 30 hypotheses for CH_4 production and oxidation, which were informed by previous studies of methane cycling in temperate ecosystems but untested in the Arctic. (1) CH_4 is produced in the more reduced subsurface, and consumed by methane



oxidizers at the upper section of the soil column where O₂ is available. (2) Methane production has higher temperature sensitivity than CH₄ oxidation, and is likely to exceed the CH₄ consumption rate in warmer temperature.

Aerobic CH₄ oxidation is usually assumed to be limited by O₂ diffusion. Therefore, near-surface layers of soil and the rhizosphere would be expected to have the highest CH₄ oxidation activity (Shukla et al., 2013; Gulledge et al., 1997). The relative abundance of the *pmoA* marker gene for CH₄ oxidation decreased with soil depth in HCP trough soils (Yang et al., 2017) and in permafrost-affected soils from the Canadian Arctic (Frank-Fahle et al., 2014), consistent with that conceptual model. Thus, we would expect that the active layers of FCP and HCP in the BEO tundra have the highest rates of CH₄ oxidation. However, the highest CH₄ oxidation potentials were measured in the transition zone and permafrost of FCP, the only layers with active methanogenesis. This result suggests that most active methanotrophs are found in these deeper soil layers.

Our results demonstrated CH₄ oxidation might not be primarily O₂ diffusion-limited, but rather limited by the availability of CH₄. The highest CH₄ oxidation potentials were measured below the rhizosphere, in suboxic layers where CH₄ has accumulated. Given that half-saturation constants for CH₄ and O₂ used in methanotrophy models vary over 1-2 orders of magnitude (Segers, 1998; Riley et al., 2011), aerobic CH₄ oxidation could occur throughout much of the soil column, as advective, diffusive or plant-mediated transport processes introduce O₂ into the soil. Others have observed deep soil CH₄ oxidation activity in peatlands (Hornibrook et al., 2009), fens (Cheema et al., 2015) and wet tundra (Barbier et al., 2012), often correlated with water table depth (Sundh et al., 1994).

The water table in the center of Barrow LCPs and FCPs varies somewhat during the thaw season but remains close to the surface (<10 cm below surface for most of the thaw season) (Liljedahl et al., 2015; Liljedahl et al., 2016). Precipitation balances evapotranspiration during the thaw season, with little lateral runoff (Dingman et al., 1980), and volumetric water contents remain constant for these features (<http://permafrostwatch.org>). In HCPs, the water table drops up to 20 cm below the surface following snowmelt (Liljedahl et al., 2015), and the soils have a lower volumetric water content. Due to limited drainage in the flat coastal plain, the frozen cores analyzed here are representative of field conditions for much of the thaw season. Water isotope analysis demonstrated that most water in the deep active layer comes from summer precipitation rather than seasonal ice melt (Throckmorton et al., 2016). Precipitation during September and October 2011 was above average for Barrow (<http://climate.gi.alaska.edu/>), suggesting a high water table during the winter freeze-up before we collected soil cores in early 2012. Cold water from precipitation mixing in the soil column could provide methanotrophs with sufficient oxygen to grow below the rhizosphere, close to the methane source. A comparison of methanogenesis and methane oxidation potential in peat bogs demonstrated that methanotrophs survived temporary exposure to anoxic conditions, suggesting these organisms can tolerate rapid changes in the water table and redox potential (Whalen and Reeburgh, 2000). These



observations argue against the hypothesis that CH₄ oxidation occurs primarily at the surface layer or at the water table interface.

Temperature disparately affects CH₄ production and oxidation, leading to a complex response in net surface-atmosphere CH₄ flux. The 4.2-fold increase in CH₄ production in the transition zone due to a 10°C rise in temperature (Q₁₀) was similar to the average value of 4.26 reported in a recent meta-analysis of permafrost-affected soils (Schädel et al., 2016). These values are substantially higher than the temperature sensitivity of CH₄ oxidation from both freshly thawed and pre-incubated samples (Q₁₀ = 2.0). While both CH₄ production and oxidation respond positively to increased temperature, CH₄ production rates are predicted to increase more rapidly with higher temperature at this critical interface between the active layer and permafrost. This difference in temperature sensitivity of CH₄ production and oxidation was also found in Arctic lakes (Lofton et al., 2014). CH₄ oxidation potential from FCP showed a temperature coefficient (Q₁₀) between 1.7 and 2.0, which is consistent with reported values from peat (Segers, 1998). Higher Q₁₀ values for CH₄ oxidation were reported in drier mineral Arctic cryosols with low organic carbon content (Jørgensen et al., 2015; Christiansen et al., 2015). When methanotrophs are located in the upper oxic portion of the soil column they should be more susceptible to changes in air temperature than methanogens in the lower anoxic soil layers. In the FCP studied here where both CH₄ production and oxidation potential are highest in the transition zone, temperature differentials should be small.

Assuming no diffusion limitation, we evaluated the net effect of CH₄ production and oxidation based on potential rate measurements from the transition zone of FCP that exhibited the highest CH₄ oxidation potential. Methane oxidation rates are 14, 9, and 7 times of the methanogenesis rate at -2, 4, and 8°C, respectively. It is quite likely that methanogenesis will outcompete CH₄ oxidation under much warmer temperature if there is no decrease in soil water content. We introduced model representations to explore this possibility, as previous studies suggest CH₄ oxidation rate is strongly regulated by the CH₄ supply (Liikanen et al., 2002; Lofton et al., 2014). By assuming zero net CH₄ production, we estimated the temperature profile of the active biomass ratio between methanogens and methanotrophs (Fig. 7). Given the large difference in the rates of CH₄ production and oxidation, CH₄ oxidation can still easily exceed CH₄ production with an active biomass ratio $B_{\text{methanotrophs}}/B_{\text{methanogens}}$ lower than 1. Studies of functional genes involved in methane production (*mcrA*) and oxidation (*pmoA*) in the active layer of four LCPs in the Western Canadian Arctic suggested substantial variation in the *pmoA/mcrA* abundance ratio; the range is between 8.5×10^{-5} and 7.6×10^2 (Frank-Fahle et al., 2014). Future investigation using molecular methods to quantify methanogen and methanotroph populations will provide better constraints. These results suggest the importance of parameterizing the temperature response function and biomass growth function specifically for methanogenesis and methane oxidation in model simulations to determine if the rates of methanogenesis and methane oxidation offset each other in the soil column.



The thawed soil incubations of FCP and HCP revealed substantial differences in the temporal dynamics of CO₂ production. An initial lag was observed from HCP samples at all temperatures, suggesting low initial microbial activity, which might be due to low moisture content, or substrate limitation. Initial active microbial biomass might also be very low given the low soil water availability. In contrast, rapid CO₂ production was observed from both active layer incubated under oxic conditions and transition zone and permafrost incubated under anoxic conditions. This temporal pattern of rapid accumulation after thawing was also observed for anaerobic respiration from LCP and HCP soils (Roy Chowdhury et al., 2015; Yang et al., 2016).

Coupled iron reduction and organic carbon oxidation processes made significant contributions to total anaerobic CO₂ production. Acetate was most abundant and exhibited the most dynamic concentration changes among individual organic acids measured from the anaerobic microcosms, which is consistent with previous studies on LCP and HCP carbon decomposition (Yang et al., 2016). The consumption of acetate correlated with increases of CH₄ and CO₂ concentrations in previous incubation experiments suggested either acetoclastic methanogenesis or syntrophic acetate oxidation coupled to hydrogenotrophic methanogenesis, which are both consistent with isotopic analyses of CH₄ from the site (Throckmorton et al., 2015; Vaughn et al., 2016). Using reaction stoichiometry for acetoclastic methanogenesis and anaerobic respiration through iron reduction (Istok et al., 2010), we estimated the amount of acetate being consumed by these parallel processes in the transition zone and permafrost (Fig. 8). In the transition zone, about half of available acetate was consumed by methanogenesis during the first 20 days of incubation, and the number dropped to about 30% during 20 to 90 days of incubation with increasing available acetate pool and increasing Fe(III) reduction. Permafrost contained a higher level of available acetate at the beginning of the incubation, and over 60% of the available acetate was rapidly consumed by Fe(III) reduction during the first 20 days of incubation. From 20 to 90 days of incubation, iron reduction still potentially consumed over half of available acetate in the permafrost. This estimation is consistent with our initial characterization of the FCP core, where the transition zone contained the highest dissolved CH₄ concentrations, and permafrost was associated with significantly higher Fe(II) concentrations (Fig. S1). If hydrogen or other organic anions such as formate or propionate were oxidized by methanogens or iron reducers, then estimated acetate production levels would decrease slightly. These simulations indicate that anaerobic iron respiration could be responsible for most of the acetate mineralized in these soil incubations.

Based on these findings, we propose the following scheme of soil carbon biogeochemistry in the FCP (Fig. 9): (1) Increasing temperature facilitates aerobic decomposition of organic carbon in the active layer, and accelerates anaerobic carbon decomposition in the lower active layer and transition zone through fermentation, iron reduction, and methanogenesis to produce CH₄ and CO₂. (2) CH₄ produced in the transition zone and permafrost is oxidized close to the site of production or transported to the atmosphere. (3) Fe(III) reduction is the primary anaerobic process responsible for the depletion of acetate, the primary SOC decomposition intermediate. In this scheme, the oxic/anoxic interface could dynamically move in the soil



column with changes in the water table and porewater distribution. Although the transition zone contained much less carbon than the permafrost layer, the total carbon loss as the sum of CO₂ and CH₄ was comparable to that from permafrost. Laboratory measurements suggested that acetate accumulated in the active layer could be transported into deeper layers to support iron reduction and methanogenesis (Yang et al., 2016). This transport might occur through vertical movement of dissolved organic compounds or mixing through cryoturbation (Drake et al., 2015).

5 Conclusions

Increased warming is predicted to accelerate the transition from wet LCPs to drier FCPs and HCPs in Arctic tundra, which probably function as potential atmospheric CH₄ sinks. This study demonstrated that CH₄ oxidation capacity was tightly linked to methane availability, rather than O₂ availability in these soils. Thus the zone of highest CH₄ oxidation potential is at the suboxic area near the FCP transition zone and the upper permafrost. The measured CH₄ oxidation potential is an order of magnitude higher than the methanogenesis rate. With higher CH₄ residence time in the soil column due to limited gas diffusion in the field, CH₄ oxidation could easily consume CH₄ produced in deep permafrost soil at warming temperature. Given that iron reduction-coupled organic carbon decomposition dominates the overall anaerobic processes, CO₂ is likely to remain the major form of carbon emission from degraded polygons. This finding provides critical information about the dynamics of CH₄ production and oxidation with increased temperature that need to be incorporated into Arctic terrestrial ecosystem models for better predictions.

Data availability

The dataset can be found in (Zheng et al., 2017).

20 Author contributions

DG, SW, and BG conceived and organized the research study; TRC, DG and SW collected core samples; JZ, TRC, ZY and performed experiments and acquired data; JZ, TRC and DG analysed and interpreted data; JZ and DG drafted the manuscript. All authors contributed revisions to the manuscript and have given approval to the final version of the manuscript.

25 Competing interests

The authors declare no competing interests.



Acknowledgments

We thank Ji-Won Moon for assistance with ion chromatography, and Bob Busey, Larry Hinzman, Kenneth Lowe and Craig Ulrich for assistance obtaining frozen core samples, as well as UMIAQ, LLC for logistical assistance. The Next-Generation Ecosystem Experiments in the Arctic (NGEE Arctic) project is supported by the Biological and Environmental Research program in the U.S. Department of Energy (DOE) Office of Science. Oak Ridge National Laboratory is managed by UT-Battelle, LLC, for the DOE under Contract No. DE-AC05-00OR22725.

References

- Barbier, B. A., Dzikuch, I., Liebner, S., Ganzert, L., Lantuit, H., Pollard, W., and Wagner, D.: Methane-cycling communities in a permafrost-affected soil on Herschel Island, Western Canadian Arctic: active layer profiling of *mcrA* and *pmoA* genes, *FEMS Microbiol. Ecol.*, 82, 287-302, <https://doi.org/10.1111/j.1574-6941.2012.01332.x>, 2012.
- Bockheim, J. G.: Importance of cryoturbation in redistributing organic carbon in permafrost-affected soils, *Soil. Sci. Soc. Am. J.*, 71, 1335-1342, <https://doi.org/10.2136/sssai2006.0414n>, 2007.
- Chang, R. Y.-W., Miller, C. E., Dinardo, S. J., Karion, A., Sweeney, C., Daube, B. C., Henderson, J. M., Mountain, M. E., Eluszkiewicz, J., Miller, J. B., Bruhwiler, L. M. P., and Wofsy, S. C.: Methane emissions from Alaska in 2012 from CARVE airborne observations, *Proc. Natl. Acad. Sci. U.S.A.*, 111, 16694-16699, <https://doi.org/10.1073/pnas.1412953111>, 2014.
- Cheema, S., Zeyer, J., and Henneberger, R.: Methanotrophic and methanogenic communities in Swiss alpine fens dominated by *Carex rostrata* and *Eriophorum angustifolium*, *Appl. Environ. Microbiol.*, 81, 5832-5844, <https://doi.org/10.1128/aem.01519-15>, 2015.
- Christiansen, J. R., Romero, A. J. B., Jørgensen, N. O. G., Glaring, M. A., Jørgensen, C. J., Berg, L. K., and Elberling, B.: Methane fluxes and the functional groups of methanotrophs and methanogens in a young Arctic landscape on Disko Island, West Greenland, *Biogeochemistry*, 122, 15-33, <https://doi.org/10.1007/s10533-014-0026-7>, 2015.
- Commam, R., Landaas, J., Benmergui, J., Luus, K. A., Chang, R. Y.-W., Daube, B. C., Euskirchen, E. S., Henderson, J. M., Karion, A., Miller, J. B., Miller, S. M., Parazoo, N. C., Randerson, J. T., Sweeney, C., Tans, P., Thoning, K., Veraverbeke, S., Miller, C. E., and Wofsy, S. C.: Carbon dioxide sources from Alaska driven by increasing early winter respiration from Arctic tundra, *Proc. Natl. Acad. Sci. U.S.A.*, 114, 5361-5366, <https://doi.org/10.1073/pnas.1618567114>, 2017.
- Dingman, S. L., Barry, R. G., Weller, G., Benson, C., LeDrew, E. F., and Goodwin, C. W.: Climate, snow cover, microclimate, and hydrology, in: *An Arctic ecosystem: the coastal tundra at Barrow, Alaska*, edited by: Brown, J., Miller, P. C., Tieszen, L. L., and Bunnell, F., Dowden, Hutchinson & Ross, Stroudsburg, PA, 30-65, 1980.
- Drake, T. W., Wickland, K. P., Spencer, R. G. M., McKnight, D. M., and Striegl, R. G.: Ancient low-molecular-weight organic acids in permafrost fuel rapid carbon dioxide production upon thaw, *Proc. Natl. Acad. Sci. U.S.A.*, 112, 13946-13951, <https://doi.org/10.1073/pnas.1511705112>, 2015.
- Frank-Fahle, B. A., Yergeau, É., Greer, C. W., Lantuit, H., and Wagner, D.: Microbial Functional Potential and Community Composition in Permafrost-Affected Soils of the NW Canadian Arctic, *PLoS ONE*, 9, e84761, <https://doi.org/10.1371/journal.pone.0084761>, 2014.
- French, H. M.: *The Periglacial Environment*, 3rd ed., John Wiley & Sons, Chichester, 2007.
- Grant, R. F., Mekonnen, Z. A., Riley, W. J., Arora, B., and Torn, M. S.: Mathematical Modelling of Arctic Polygonal Tundra with *Ecosys*: 2. Microtopography Determines How CO₂ and CH₄ Exchange Responds to Changes in Temperature and Precipitation, *Journal of Geophysical Research: Biogeosciences*, n/a-n/a, <https://doi.org/10.1002/2017JG004037>, 2017.
- Gulledge, J., Doyle, A. P., and Schimel, J. P.: Different NH₄⁺-inhibition patterns of soil CH₄ consumption: A result of distinct CH₄-oxidizer populations across sites?, *Soil Biol. Biochem.*, 29, 13-21, [https://doi.org/10.1016/S0038-0717\(96\)00265-9](https://doi.org/10.1016/S0038-0717(96)00265-9), 1997.
- Herndon, E. M., Mann, B. F., Roy Chowdhury, T., Yang, Z., Wulfschleger, S. D., Graham, D., Liang, L., and Gu, B.: Pathways of anaerobic organic matter decomposition in tundra soils from Barrow, Alaska, *J. Geophys. Res.-Biogeo.*, 120, 2345-2359, <https://doi.org/10.1002/2015JG003147>, 2015a.
- Herndon, E. M., Yang, Z., Bargar, J., Janot, N., Regier, T. Z., Graham, D. E., Wulfschleger, S. D., Gu, B., and Liang, L.: Geochemical drivers of organic matter decomposition in arctic tundra soils, *Biogeochemistry*, 126, 397-414, <https://doi.org/10.1007/s10533-015-0165-5>, 2015b.



- Hornibrook, E. R. C., Bowes, H. L., Culbert, A., and Gallego-Sala, A. V.: Methanotrophy potential versus methane supply by pore water diffusion in peatlands, *Biogeosciences*, 6, 1491-1504, <https://doi.org/10.5194/bg-6-1491-2009>, 2009.
- Howeler, R. H., and Bouldin, D. R.: The Diffusion and Consumption of Oxygen in Submerged Soils, *Soil. Sci. Soc. Am. J.*, 35, 202-208, <https://doi.org/10.2136/sssaj1971.03615995003500020014x>, 1971.
- 5 Hugelius, G., Strauss, J., Zubrzycki, S., Harden, J. W., Schuur, E. A. G., Ping, C. L., Schirmer, L., Grosse, G., Michaelson, G. J., Koven, C. D., O'Donnell, J. A., Elberling, B., Mishra, U., Camill, P., Yu, Z., Palmtag, J., and Kuhry, P.: Estimated stocks of circumpolar permafrost carbon with quantified uncertainty ranges and identified data gaps, *Biogeosciences*, 11, 6573-6593, <https://doi.org/10.5194/bg-11-6573-2014>, 2014.
- 10 Istok, J. D., Park, M., Michalsen, M., Spain, A. M., Krumholz, L. R., Liu, C., McKinley, J., Long, P., Roden, E., Peacock, A. D., and Baldwin, B.: A thermodynamically-based model for predicting microbial growth and community composition coupled to system geochemistry: Application to uranium bioreduction, *J. Contam. Hydrol.*, 112, 1-14, <https://doi.org/10.1016/j.jconhyd.2009.07.004>, 2010.
- Jørgensen, C. J., Lund Johansen, K. M., Westergaard-Nielsen, A., and Elberling, B.: Net regional methane sink in High Arctic soils of northeast Greenland, *Nature Geosci.*, 8, 20-23, <https://doi.org/10.1038/ngeo2305>, 2015.
- 15 Knoblauch, C., Spott, O., Evgrafova, S., Kutzbach, L., and Pfeiffer, E.-M.: Regulation of methane production, oxidation, and emission by vascular plants and bryophytes in ponds of the northeast Siberian polygonal tundra, *J. Geophys. Res.-Biogeo.*, 120, 2525-2541, <https://doi.org/10.1002/2015JG003053>, 2015.
- Laanbroek, H. J.: Methane emission from natural wetlands: interplay between emergent macrophytes and soil microbial processes. A mini-review, *Annals of botany*, 105, 141-153, <https://doi.org/10.1093/aob/mcp201>, 2010.
- 20 Langford, Z., Kumar, J., Hoffman, F., Norby, R., Wullschlegel, S., Sloan, V., and Iversen, C.: Mapping Arctic Plant Functional Type Distributions in the Barrow Environmental Observatory Using WorldView-2 and LiDAR Datasets, *Remote Sensing*, 8, 733, <https://doi.org/10.3390/rs8090733>, 2016.
- Lara, M. J., McGuire, A. D., Euskirchen, E. S., Tweedie, C. E., Hinkel, K. M., Skurikhin, A. N., Romanovsky, V. E., Grosse, G., Bolton, W. R., and Genet, H.: Polygonal tundra geomorphological change in response to warming alters future CO₂ and CH₄ flux on the Barrow Peninsula, *Glob. Change Biol.*, 21, 1634-1651, <https://doi.org/10.1111/gcb.12757>, 2015.
- 25 Lau, M. C. Y., Stackhouse, B. T., Layton, A. C., Chauhan, A., Vishnivetskaya, T. A., Chourey, K., Ronholm, J., Mykietczuk, N. C. S., Bennett, P. C., Lamarche-Gagnon, G., Burton, N., Pollard, W. H., Omelon, C. R., Medvigy, D. M., Hettich, R. L., Piffner, S. M., Whyte, L. G., and Onstott, T. C.: An active atmospheric methane sink in high Arctic mineral cryosols, *ISME J.*, 9, 1880-1891, <https://doi.org/10.1038/ismej.2015.13>, 2015.
- 30 Le Mer, J., and Roger, P.: Production, oxidation, emission and consumption of methane by soils: A review, *Eur. J. Soil Biol.*, 37, 25-50, [https://doi.org/10.1016/s1164-5563\(01\)01067-6](https://doi.org/10.1016/s1164-5563(01)01067-6), 2001.
- Lee, H. J., Jeong, S. E., Kim, P. J., Madsen, E. L., and Jeon, C. O.: High resolution depth distribution of Bacteria, Archaea, methanotrophs, and methanogens in the bulk and rhizosphere soils of a flooded rice paddy, *Front. Microbiol.*, 6, <https://doi.org/10.3389/fmicb.2015.00639>, 2015.
- 35 Liebner, S., Schwarzenbach, S. P., and Zeyer, J.: Methane emissions from an alpine fen in central Switzerland, *Biogeochemistry*, 109, 287-299, <https://doi.org/10.1007/s10533-011-9629-4>, 2012.
- Liikanen, A., Huttunen, J. T., Valli, K., and Martikainen, P. J.: Methane cycling in the sediment and water column of mid-boreal hyper-eutrophic Lake Kevätön, Finland, *Ark. Hydrobiol.*, 154, 585-603, <https://doi.org/10.1127/archiv-hydrobiol/154/2002/585>, 2002.
- 40 Liljedahl, A. K., Wilson, C., Kholodov, A., Chamberlain, A., Lee, H., Daanen, R., Cohen, L., Hayes, S., Iwahana, G., Iversen, A., Weiss, T., Hoffman, A., Wullschlegel, S., and Hinzman, L.: Ground Water Levels for NGEE Areas A, B, C and D, Barrow, Alaska, 2012-2014, Accessed at <https://doi.org/10.5440/1183767>, 2015.
- Liljedahl, A. K., Boike, J., Daanen, R. P., Fedorov, A. N., Frost, G. V., Grosse, G., Hinzman, L. D., Iijma, Y., Jorgenson, J. C., Matveyeva, N., Necsoiu, M., Reynolds, M. K., Romanovsky, V. E., Schulla, J., Tape, K. D., Walker, D. A., Wilson, C. J., Yabuki, H., and Zona, D.: Pan-Arctic ice-wedge degradation in warming permafrost and its influence on tundra hydrology, *Nature Geosci.*, 9, 312-318, <https://doi.org/10.1038/ngeo2674>, 2016.
- 45 Lofton, D. D., Whalen, S. C., and Hershey, A. E.: Effect of temperature on methane dynamics and evaluation of methane oxidation kinetics in shallow Arctic Alaskan lakes, *Hydrobiologia*, 721, 209-222, <https://doi.org/10.1007/s10750-013-1663-x>, 2014.
- MacKay, J. R.: Thermally induced movements in ice-wedge polygons, western arctic coast: a long-term study, *Geographie physique et Quaternaire*, 54, 41-68, <https://doi.org/10.7202/004846ar>, 2000.
- 50 McGuire, A. D., Christensen, T. R., Hayes, D., Heroult, A., Euskirchen, E., Kimball, J. S., Koven, C., Lafleur, P., Miller, P. A., Oechel, W., Peylin, P., Williams, M., and Yi, Y.: An assessment of the carbon balance of Arctic tundra: comparisons among observations, process models, and atmospheric inversions, *Biogeosciences*, 9, 3185-3204, <https://doi.org/10.5194/bg-9-3185-2012>, 2012.



- Parmentier, F. J. W., van Huissteden, J., Kip, N., Op den Camp, H. J. M., Jetten, M. S. M., Maximov, T. C., and Dolman, A. J.: The role of endophytic methane-oxidizing bacteria in submerged *Sphagnum* in determining methane emissions of Northeastern Siberian tundra, *Biogeosciences*, 8, 1267-1278, <https://doi.org/10.5194/bg-8-1267-2011>, 2011.
- Preuss, I., Knoblauch, C., Gebert, J., and Pfeiffer, E. M.: Improved quantification of microbial CH₄ oxidation efficiency in arctic wetland soils using carbon isotope fractionation, *Biogeosciences*, 10, 2539-2552, <https://doi.org/10.5194/bg-10-2539-2013>, 2013.
- Raz-Yaseef, N., Torn, M. S., Wu, Y., Billesbach, D. P., Liljedahl, A. K., Kneafsey, T. J., Romanovsky, V. E., Cook, D. R., and Wullschleger, S. D.: Large CO₂ and CH₄ emissions from polygonal tundra during spring thaw in northern Alaska, *Geophys. Res. Lett.*, 44, 504-513, <https://doi.org/10.1002/2016GL071220>, 2017.
- Riley, W. J., Subin, Z. M., Lawrence, D. M., Swenson, S. C., Torn, M. S., Meng, L., Mahowald, N. M., and Hess, P.: Barriers to predicting changes in global terrestrial methane fluxes: analyses using CLM4Me, a methane biogeochemistry model integrated in CESM, *Biogeosciences*, 8, 1925-1953, <https://doi.org/10.5194/bg-8-1925-2011>, 2011.
- Romanovsky, V. E., and Osterkamp, T. E.: Effects of unfrozen water on heat and mass transport processes in the active layer and permafrost, *Permafrost Periglac.*, 11, 219-239, [https://doi.org/10.1002/1099-1530\(200007/09\)11:3<219::aid-ppp352>3.0.co;2-7](https://doi.org/10.1002/1099-1530(200007/09)11:3<219::aid-ppp352>3.0.co;2-7), 2000.
- Roslev, P., and King, G. M.: Regulation of methane oxidation in a freshwater wetland by water table changes and anoxia, *FEMS Microbiol. Ecol.*, 19, 105-115, [https://doi.org/10.1016/0168-6496\(95\)00084-4](https://doi.org/10.1016/0168-6496(95)00084-4), 1996.
- Roy Chowdhury, T., Mitsch, W. J., and Dick, R. P.: Seasonal methanotrophy across a hydrological gradient in a freshwater wetland, *Ecol. Eng.*, 72, 116-124, <https://doi.org/http://dx.doi.org/10.1016/j.ecoleng.2014.08.015>, 2014.
- Roy Chowdhury, T., Herndon, E. M., Phelps, T. J., Elias, D. A., Gu, B., Liang, L., Wullschleger, S. D., and Graham, D. E.: Stoichiometry and temperature sensitivity of methanogenesis and CO₂ production from saturated polygonal tundra in Barrow, Alaska, *Glob. Change Biol.*, 21, 722-737, <https://doi.org/10.1111/gcb.12762>, 2015.
- Sachs, T., Giebels, M., Boike, J., and Kutzbach, L.: Environmental controls on CH₄ emission from polygonal tundra on the microsite scale in the Lena river delta, Siberia, *Glob. Change Biol.*, 16, 3096-3110, <https://doi.org/10.1111/j.1365-2486.2010.02232.x>, 2010.
- Sander, R.: Compilation of Henry's law constants (version 4.0) for water as solvent, *Atmos. Chem. Phys.*, 15, 4399-4981, <https://doi.org/10.5194/acp-15-4399-2015>, 2015.
- Schädel, C., Bader, M. K. F., Schuur, E. A. G., Biasi, C., Bracho, R., Capek, P., De Baets, S., Diakova, K., Ernakovich, J., Estop-Aragones, C., Graham, D. E., Hartley, I. P., Iversen, C. M., Kane, E., Knoblauch, C., Lupascu, M., Martikainen, P. J., Natali, S. M., Norby, R. J., O'Donnell, J. A., Chowdhury, T. R., Santruckova, H., Shaver, G., Sloan, V. L., Treat, C. C., Turetsky, M. R., Waldrop, M. P., and Wickland, K. P.: Potential carbon emissions dominated by carbon dioxide from thawed permafrost soils, *Nature Clim. Change*, 6, 950-953, <https://doi.org/10.1038/nclimate3054>, 2016.
- Schuur, E. A. G., Bockheim, J., Canadell, J. G., Euskirchen, E., Field, C. B., Goryachkin, S. V., Hagemann, S., Kuhry, P., Lafleur, P. M., Lee, H., Mazhitova, G., Nelson, F. E., Rinke, A., Romanovsky, V. E., Shiklomanov, N., Tarnocai, C., Venevsky, S., Vogel, J. G., and Zimov, S. A.: Vulnerability of permafrost carbon to climate change: implications for the global carbon cycle, *BioScience*, 58, 701-714, <https://doi.org/10.1641/b580807>, 2008.
- Schuur, E. A. G., Abbott, B. W., Bowden, W. B., Brovkin, V., Camill, P., Canadell, J. G., Chanton, J. P., Chapin, F. S., Christensen, T. R., Ciais, P., Crosby, B. T., Czimeczik, C. I., Grosse, G., Harden, J., Hayes, D. J., Hugelius, G., Jastrow, J. D., Jones, J. B., Kleinen, T., Koven, C. D., Krinner, G., Kuhry, P., Lawrence, D. M., McGuire, A. D., Natali, S. M., O'Donnell, J. A., Ping, C. L., Riley, W. J., Rinke, A., Romanovsky, V. E., Sannel, A. B. K., Schädel, C., Schaefer, K., Sky, J., Subin, Z. M., Tarnocai, C., Turetsky, M. R., Waldrop, M. P., Walter Anthony, K. M., Wickland, K. P., Wilson, C. J., and Zimov, S. A.: Expert assessment of vulnerability of permafrost carbon to climate change, *Climatic Change*, 119, 359-374, <https://doi.org/10.1007/s10584-013-0730-7>, 2013.
- Schuur, E. A. G., McGuire, A. D., Schädel, C., Grosse, G., Harden, J. W., Hayes, D. J., Hugelius, G., Koven, C. D., Kuhry, P., Lawrence, D. M., Natali, S. M., Olefeldt, D., Romanovsky, V. E., Schaefer, K., Turetsky, M. R., Treat, C. C., and Vonk, J. E.: Climate change and the permafrost carbon feedback, *Nature*, 520, 171-179, <https://doi.org/10.1038/nature14338>, 2015.
- Segers, R.: Methane production and methane consumption: a review of processes underlying wetland methane fluxes, *Biogeochemistry*, 41, 23-51, <https://doi.org/10.1023/A:100592903>, 1998.
- Shiklomanov, N. I., Streletskiy, D. A., Nelson, F. E., Hollister, R. D., Romanovsky, V. E., Tweedie, C. E., Bockheim, J. G., and Brown, J.: Decadal variations of active-layer thickness in moisture-controlled landscapes, Barrow, Alaska, *J. Geophys. Res.-Biogeo.*, 115, G00I04, <https://doi.org/10.1029/2009JG001248>, 2010.
- Shukla, P. N., Pandey, K. D., and Mishra, V. K.: Environmental Determinants of Soil Methane Oxidation and Methanotrophs, *Crit. Rev. Environ. Sci. Technol.*, 43, 1945-2011, <https://doi.org/10.1080/10643389.2012.672053>, 2013.
- Sturtevant, C. S., Oechel, W. C., Zona, D., Kim, Y., and Emerson, C. E.: Soil moisture control over autumn season methane flux, Arctic Coastal Plain of Alaska, *Biogeosciences*, 9, 1423-1440, <https://doi.org/10.5194/bg-9-1423-2012>, 2012.
- Sturtevant, C. S., and Oechel, W. C.: Spatial variation in landscape-level CO₂ and CH₄ fluxes from arctic coastal tundra: influence from vegetation, wetness, and the thaw lake cycle, *Glob. Change Biol.*, 19, 2853-2866, <https://doi.org/10.1111/gcb.12247>, 2013.



- Sundh, I., Nilsson, M., Granberg, G., and Svensson, B. H.: Depth distribution of microbial production and oxidation of methane in northern boreal peatlands, *Microb. Ecol.*, 27, 253-265, <https://doi.org/10.1007/bf00182409>, 1994.
- Throckmorton, H. M., Heikoop, J. M., Newman, B. D., Altmann, G. L., Conrad, M. S., Muss, J. D., Perkins, G. B., Smith, L. J., Torn, M. S., Wullschleger, S. D., and Wilson, C. J.: Pathways and transformations of dissolved methane and dissolved inorganic carbon in Arctic tundra watersheds: Evidence from analysis of stable isotopes, *Global Biogeochem. Cy.*, 29, 1893-1910, <https://doi.org/10.1002/2014GB005044>, 2015.
- Throckmorton, H. M., Newman, B. D., Heikoop, J. M., Perkins, G. B., Feng, X., Graham, D. E., O'Malley, D., Vesselinov, V. V., Young, J., Wullschleger, S. D., and Wilson, C. J.: Active layer hydrology in an arctic tundra ecosystem: quantifying water sources and cycling using water stable isotopes, *Hydrological Processes*, 30, 4972-4986, <https://doi.org/10.1002/hyp.10883>, 2016.
- Treat, C. C., Natali, S. M., Ernakovich, J., Iversen, C. M., Lupascu, M., McGuire, A. D., Norby, R. J., Roy Chowdhury, T., Richter, A., Šantrůčková, H., Schädel, C., Schuur, E. A. G., Sloan, V. L., Turetsky, M. R., and Waldrop, M. P.: A pan-Arctic synthesis of CH₄ and CO₂ production from anoxic soil incubations, *Glob. Change Biol.*, 21, 2787-2803, <https://doi.org/10.1111/gcb.12875>, 2015.
- Vaughn, L. J. S., Conrad, M. E., Bill, M., and Torn, M. S.: Isotopic insights into methane production, oxidation, and emissions in Arctic polygon tundra, *Glob. Change Biol.*, 22, 3487-3502, <https://doi.org/10.1111/gcb.13281>, 2016.
- von Fischer, J. C., Rhew, R. C., Ames, G. M., Fosdick, B. K., and von Fischer, P. E.: Vegetation height and other controls of spatial variability in methane emissions from the Arctic coastal tundra at Barrow, Alaska, *J. Geophys. Res.-Biogeo.*, 115, G00I03, <https://doi.org/10.1029/2009jg001283>, 2010.
- Wainwright, H. M., Dafflon, B., Smith, L. J., Hahn, M. S., Curtis, J. B., Wu, Y., Ulrich, C., Peterson, J. E., Torn, M. S., and Hubbard, S. S.: Identifying multiscale zonation and assessing the relative importance of polygon geomorphology on carbon fluxes in an Arctic tundra ecosystem, *Journal of Geophysical Research: Biogeosciences*, 120, 788-808, <https://doi.org/10.1002/2014JG002799>, 2015.
- Whalen, S. C., and Reeburgh, W. S.: Methane Oxidation, Production, and Emission at Contrasting Sites in a Boreal Bog, *Geomicrobiol. J.*, 17, 237-251, <https://doi.org/10.1080/01490450050121198>, 2000.
- Xu, X., Elias, D. A., Graham, D. E., Phelps, T. J., Carroll, S. L., Wullschleger, S. D., and Thornton, P. E.: A microbial functional group-based module for simulating methane production and consumption: Application to an incubated permafrost soil, *J. Geophys. Res.-Biogeo.*, 120, 1315-1333, <https://doi.org/10.1002/2015JG002935>, 2015.
- Yang, Z., Wullschleger, S. D., Liang, L., Graham, D. E., and Gu, B.: Effects of warming on the degradation and production of low-molecular-weight labile organic carbon in an Arctic tundra soil, *Soil Biol. Biochem.*, 95, 202-211, <https://doi.org/http://dx.doi.org/10.1016/j.soilbio.2015.12.022>, 2016.
- Yang, Z., Yang, S., Van Nostrand, J. D., Zhou, J., Fang, W., Qi, Q., Liu, Y., Wullschleger, S. D., Liang, L., Graham, D. E., Yang, Y., and Gu, B.: Microbial Community and Functional Gene Changes in Arctic Tundra Soils in a Microcosm Warming Experiment, *Front. Microbiol.*, 8, 1741, <https://doi.org/10.3389/fmicb.2017.01741>, 2017.
- Zheng, J., RoyChowdhury, T., and Graham, D. E.: CO₂ and CH₄ Production and CH₄ Oxidation in Low Temperature Soil Incubations from Flat- and High-Centered Polygons, Barrow, Alaska, 2012, Accessed at <https://doi.org/10.5440/1288688>, 2017.
- Zona, D., Gioli, B., Commane, R., Lindaas, J., Wofsy, S. C., Miller, C. E., Dinardo, S. J., Dengel, S., Sweeney, C., Karion, A., Chang, R. Y.-W., Henderson, J. M., Murphy, P. C., Goodrich, J. P., Moreaux, V., Liljedahl, A., Watts, J. D., Kimball, J. S., Lipson, D. A., and Oechel, W. C.: Cold season emissions dominate the Arctic tundra methane budget, *Proc. Natl. Acad. Sci. U.S.A.*, 113, 40-45, <https://doi.org/10.1073/pnas.1516017113>, 2016.

40

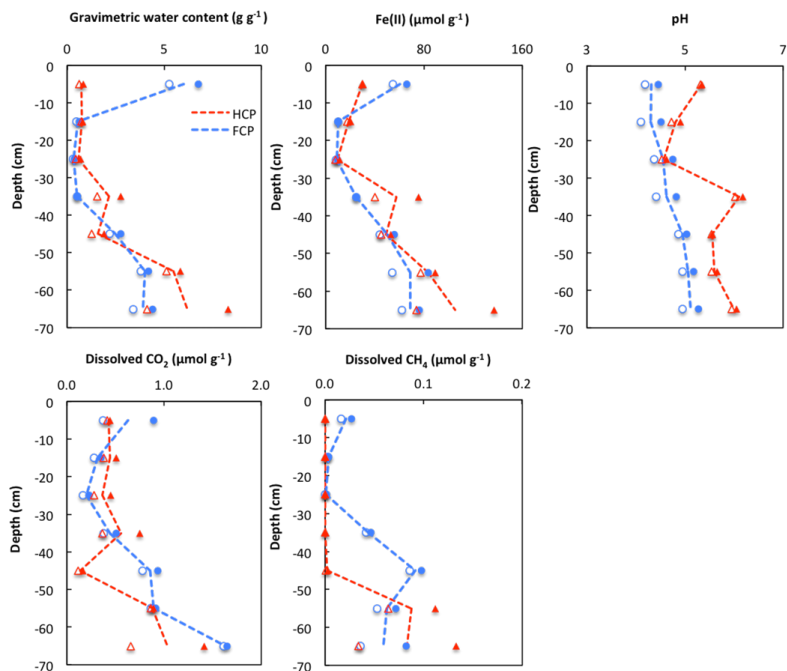
**Table 1.** Concentrations of Organic Acids* from FCP Transition Zone and Permafrost

	Incubation days	FCP Transition Zone			FCP Permafrost		
		-2°C	4°C	8°C	-2°C	4°C	8°C
Formate	0		0.68			1.68	
	20	0.77	0.72	0.86	1.56	1.43	1.96
	90	0.48±0.06	0.52±0.02	0.44±0.07	0.99±0.2	1.04±0.24	1.14±0.05
Acetate	0		1.28			10.97	
	20	1.44	1.76	1.89	10.95	9.78	12.94
	90	2.00±0.44	3.10±0.02	3.27±0.07	12.79±1.18	15.29±0.75	16.78±2.92
Propionate	0		0.49			3.82	
	20	0.53	0.65	0.62	3.73	2.97	3.82
	90	0.51±0.12	0.51±0.03	0.39±0.06	8.9±0.33	8.8±0.18	10.1±0.41
Butyrate	0		0.10			1.74	
	20	0.12	0.16	0.20	1.87	1.64	2.13
	90	0.08±0.02	0.15±0.01	0.11±0.03	1.92±0.11	2.11±0.07	2.17±0.13
Oxalate	0		0.09			0.23	
	20	0.12	0.14	0.16	0.28	0.31	0.34
	90	0.10±0.02	0.11±0.00	0.08±0.01	0.23±0.03	0.24±0.03	0.26±0.01

*Results are presented in $\mu\text{mol g}^{-1}$ (on a soil dry mass basis). The average and standard deviation are shown for triplicate microcosms incubated for 90 days.

5

10



5 **Fig. 1.** Depth profile of gravimetric water content, Fe(II) concentration, pH and soil pore water dissolved CO₂ and CH₄ concentrations from FCP (blue) and HCP (red) cores. Replicate measurements were plotted as high and low values in each soil section as filled and empty circles (FCP) and triangles (HCP). Trend lines were plotted based on the averaged value of high and low.

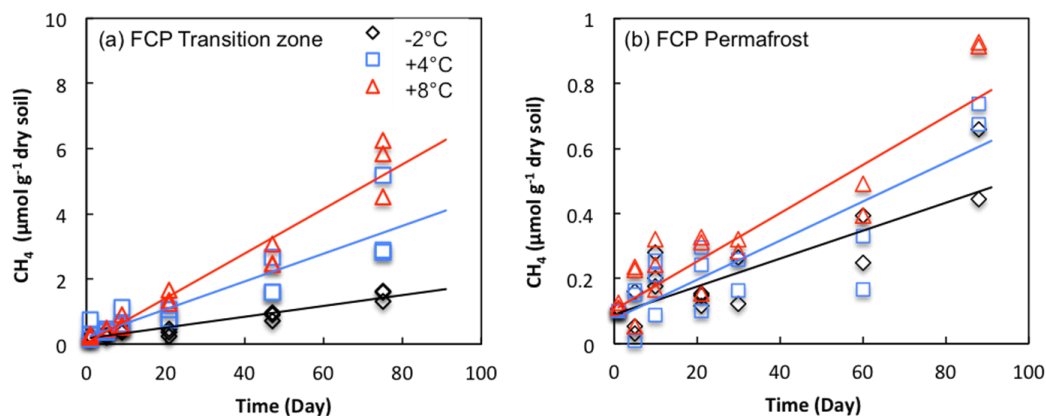


Fig. 2. CH_4 production in anoxic soil microcosms from (a) transition zone, and (b) permafrost of the FCP at indicated temperature. Cumulative CH_4 production was standardized to dry soil mass.

5

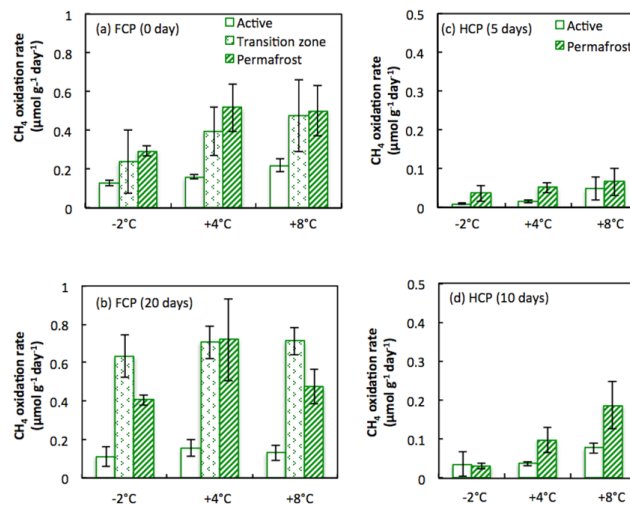


Fig. 3. CH_4 oxidation potential measured from soils incubated at the indicated temperatures from (a) FCP after 0 days, (b) FCP after 20 days, (c) HCP after 5 days, and (d) HCP after 10 days. Error bars are ± 1 sample standard deviation from the mean of three replicate incubations. Cumulative CH_4 oxidation was standardized to dry soil mass.

10

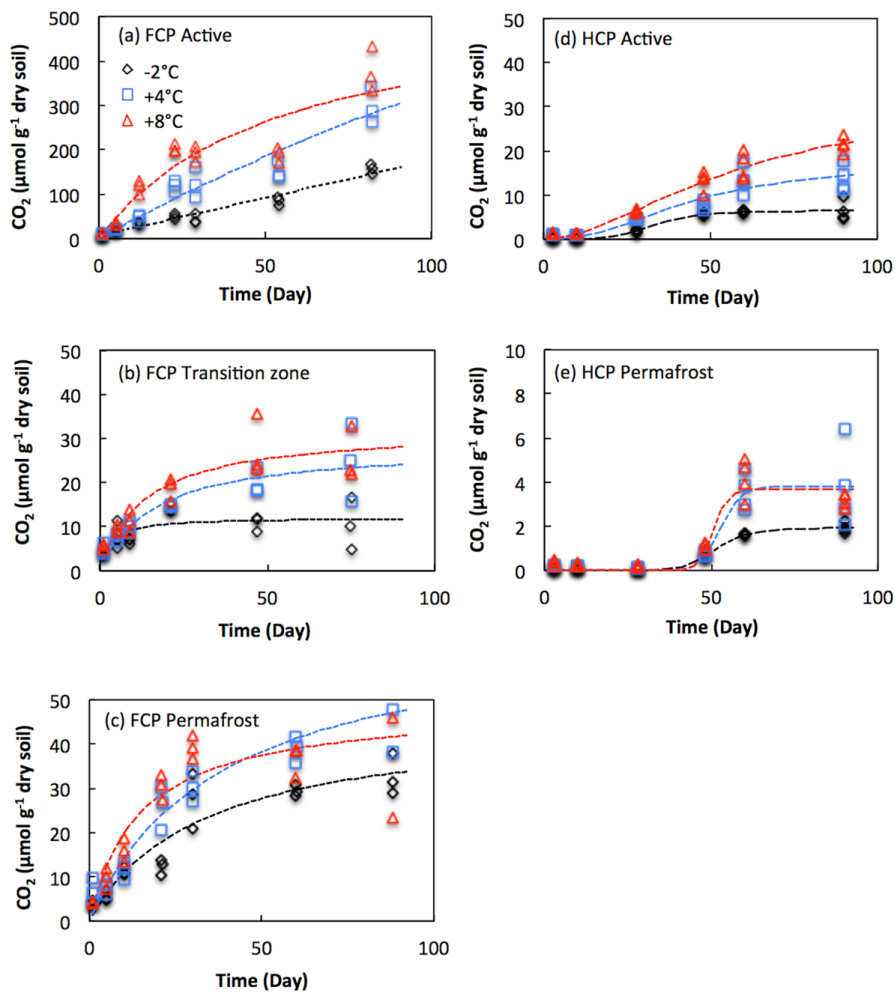


Fig. 4. Cumulative CO₂ production in soil microcosms from (a) active layer, (b) transition zone, and (c) permafrost of the FCP center core and (d) active and (e) permafrost layers of the HCP center core. No transition zone was identified in the HCP core.

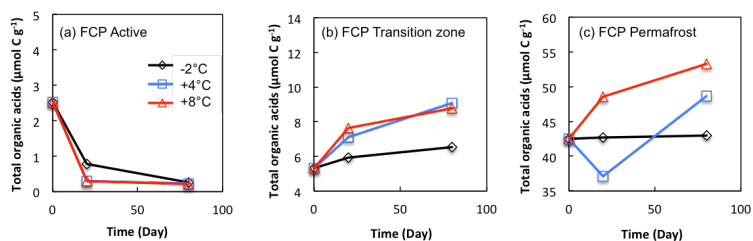
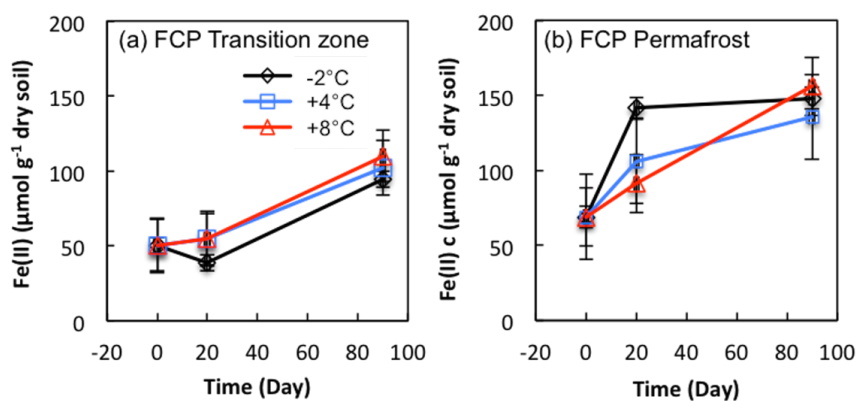


Fig. 5. Changes in total organic acids (T_{OA}) in soil microcosms from (a) active layer, (b) transition zone and (c) permafrost of FCP. Total organic acids ($\mu\text{mol C g}^{-1}$) were calculated from the concentrations of individual organic acids (Table 1).



5

Fig. 6. Changes in Fe(II) concentrations from (a) transition zone and (b) permafrost of FCP during anoxic incubations. Error bars are ± 1 standard deviation from three replicate incubations.

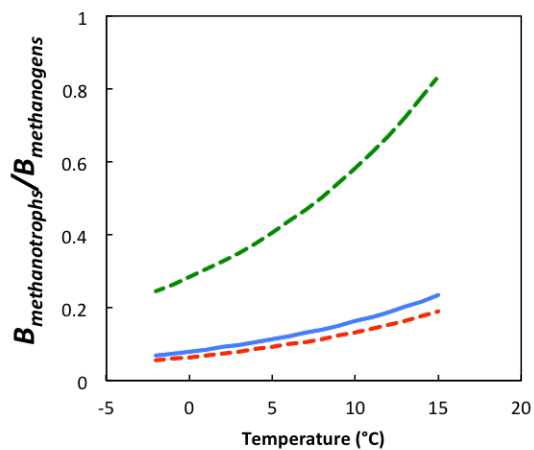


Fig. 7. Active biomass ratio $B_{\text{methanotrophs}}/B_{\text{methanogens}}$ needed for zero net CH_4 emission at different temperature. Dissolved CH_4 and O_2 concentrations in soil pore water are assumed to be 0.1mM. Half saturation rates (K_{m,CH_4} and K_{m,O_2}) represent the baseline value (Blue), high (Green) and low (Red) range for sensitivity analysis.

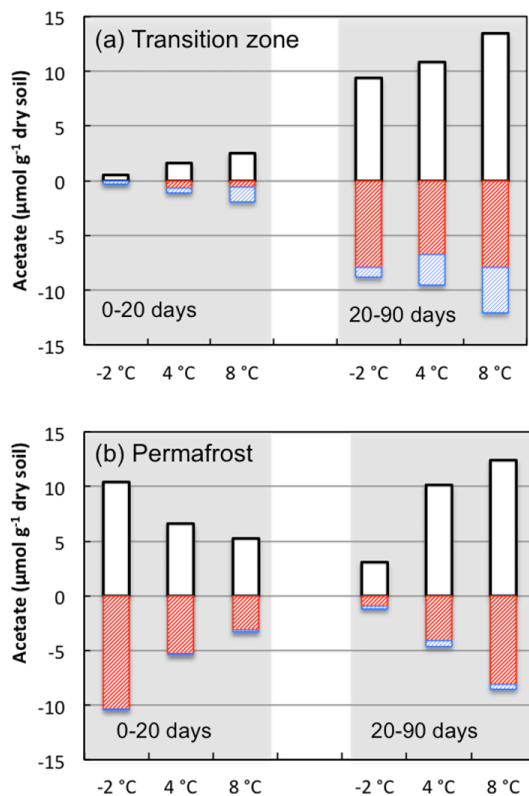


Fig. 8. Acetate production (white bars) and consumption by iron reducing bacteria (red bars) or methanogens (blue bars) were estimated using stoichiometric calculations based on measurements of methane and Fe(II) during incubations from 0 to 20 days and from 20 to 90 days at the indicated incubation temperatures.

5

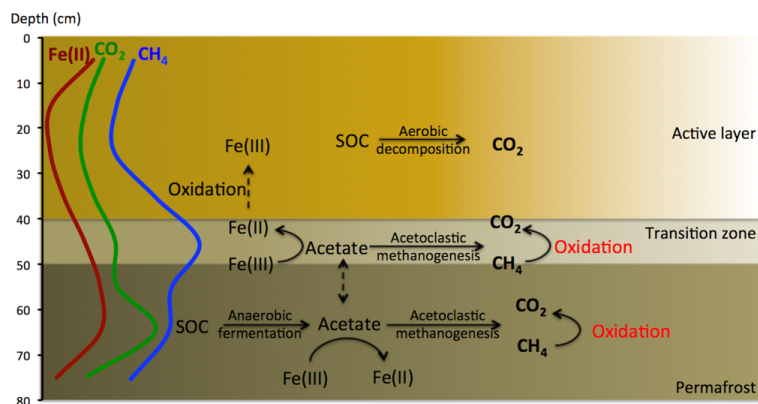


Fig. 9. Conceptual model of aerobic and anaerobic soil organic carbon decomposition pathways and the release of CO_2 and CH_4 from a flat-centered polygon. Lines on the left marked as Fe(II), CO_2 , and CH_4 represent qualitative gradients through the soil column. The median height of the water table in FCP centers is at the ground surface, with a standard deviation of ± 7 cm during the thaw season (Liljedahl et al., 2015).

5